Electric Power Systems Research 195 (2021) 107170

Contents lists available at ScienceDirect

Electric Power Systems Research

journal homepage: www.elsevier.com/locate/epsr

Optimal sizing of battery energy storage in a microgrid considering capacity degradation and replacement year

Mohammad Amini [a], Amir Khorsandi [*,a], Behrooz Vahidi [a], Seyed Hossein Hosseinian [a], Ali Malakmahmoudi [a]

Department of Electrical Engineering, Amirkabir University of Technology (Tehran Polytechnic), Iran

ARTICLE INFO

Keywords:
Battery energy storage (BES)
optimal sizing
microgrid
BES replacement
BES capacity degradation

ABSTRACT

Nowadays, microgrids (MGs) have received significant attention. In a cost-effective MG, battery energy storage (BES) plays an important role. One of the most important challenges in the MGs is the optimal sizing of the BES that can lead to the MG better performance, more flexible, effective, and efficient than traditional power systems. This paper proposes a novel set of formulations to determine the optimal BES size, technology, depth of discharge (DOD), and replacement year considering its technical characteristics, service life, and capacity degradation to minimize the MG scheduling total cost and improve the precision and economic feasibility of the BES sizing method. Moreover, the modeling of BES considering capacity degradation is presented. The proposed model of the planning problem is formulated using mixed-integer linear programming (MILP) to ensure the convergence of the optimization problem. The effectiveness of the proposed approach is confirmed by numerical simulation based on historical data of a real MG.

1. Introduction

The enhancing demand and population growth in recent years have led to a considerable increase in the development of renewable energy generators in the electricity grid [1]. The increasing of distributed generation (DG) resources, which are mostly installed at the distribution level, created small power grids called microgrid (MG). A comprehensive definition for MG by the U.S. Department of Energy (DOE) is presented in [2]. Most DG resources are naturally intermittent. On the other hand, the amount of consumed electricity by consumers varies at different times of the day; thus, balance keeping between the generation and load is one of the most essential MG challenges. Different solutions have been employed to solve this challenge including energy storage system (ESS), load shifting, load shedding, and interconnection to the utility grid. Among all of the solutions, ESS installation along with the DG resources and consumers has received more attention [3]. ESS has some attractive functions to enhance the operation of the power network and ensure load balancing including peak shaving, power quality and reliability improvement, and mitigation of the intermittent nature of renewable energy resources [4].

Several types of ESS technologies have been applied in MG applications that among of them, batteries have gained more consideration [5]. The optimal battery energy storage (BES) sizing for MG applications is a complicated problem. Some authors have discussed the problem of optimal energy storage system sizing with various levels of details and various optimization techniques. In [6], a new method is introduced for optimal BES sizing in the MG to decrease the operation cost. In [7], the optimization problem of BES sizing using particle swarm optimization (PSO), including demand response, is proposed to improve the stability of the MG frequency control.

The load uncertainty for enhancing the reliability of a MG is investigated in [8], where the objective function is the minimization of the total cost via BES. In [9], the optimal size of ESS is calculated to improve the power quality in the MG. The optimal selection of capacity and placement of BES and photovoltaic (PV) generation is examined in [10] to improve the system resilience due to the extreme events. In [11], a novel algorithm is proposed to determine the best siting of ESS in the transmission network to decrease the daily energy generation cost. The optimization of BES sizing in three scenarios for connected and islanded MG based on the operation cost is analyzed in [12]; however, the optimal BES replacement year and capacity degradation are ignored. The optimal selection of BES technologies is presented in [13]. The BES,

* Corresponding author.
E-mail addresses: mohammad.amini@aut.ac.ir (M. Amini), a_khorsandi@aut.ac.ir (A. Khorsandi), vahidi@aut.ac.ir (B. Vahidi), hosseinian@aut.ac.ir (S.H. Hosseinian), ali_malak@aut.ac.ir (A. Malakmahmoudi).

https://doi.org/10.1016/j.epsr.2021.107170
Received 10 September 2020; Received in revised form 8 February 2021; Accepted 11 March 2021
Available online 22 March 2021

smart lighting load, and PV are used to improve frequency control and reduce BES size in [14]; however, the BES service life and capacity degradation are ignored. In [15], a cost-benefit optimization approach for distributed BES is presented under high PV penetration for voltage regulation and peak load shaving. A MG planning method is proposed in [16] to determine the optimal production of distributed energy resource (DER) and type of MG; however, the BES technical characteristics are neglected.

In [17], a novel method is proposed to calculate the optimal siting and sizing of ESS for grid support. In [18], a novel control method is proposed to increase the power availability of BES. A novel mathematical formulation to investigate the role of the BES in a distribution system is presented in [19]; however, the optimal BES replacement year and the relationship between DOD and cycle life to determine the optimal BES size are ignored. In [20], a new algorithm for calculation of BES sizing for intelligent photovoltaic (IPV) power plant is presented to increase the economic benefits. In [21], a bi-level model is presented to determine the optimal size of BES based on the maximization of benefit; however, the capacity degradation is ignored. Also, in [22], a BES control strategy is used for the participation of wind farms in electricity markets.

A new nonlinear algorithm to increase the BES economic benefits in the ancillary service market, considering the BES capacity degradation process is presented in [23]; however, the effect of the BES capacity degradation on the optimization problem to determine the optimal BES size is neglected. According to the effect of stress factors on BES capacity degradation, a novel accelerated testing to model and analyze the BES capacity degradation process is introduced in [24]; however, due to the complexity and non-linearity of the proposed model the computation time is considerably increases, and also the effect of the stress factors to calculate the optimal BES size is neglected. Moreover, a non-linear planning model could be stuck in a locally optimum solution. In [25], an optimal planning method of grid-connected MG considering the BES cycle life has been proposed, however the BES float life has not been considered. In [26], a novel nonlinear method for optimal sizing of BES is proposed in islanding MG with fix replacement year; however, the optimal BES replacement year and DOD have not been considered. In [27] a novel method is presented to determine the optimal BES size and energy management for hybrid electric vehicles. Also, the effect of the DOD on the BES energy management is considered; however, the relation between the BES cycle life and DOD to the calculate optimal DOD is neglected. A non-linearized BES sizing model for shipboard considering BES cycle life is proposed in [28]; however, the optimal DOD and economic feasibility for BES replacement are ignored. In [29], a comprehensive optimal BES sizing for a MG is investigated, but the BES float life, replacement year, and capacity degradation are neglected. A new droop control method based on the incremental cost and the output voltage of the BES is proposed in [30] for islanded DC microgrid to decrease the BES degradation cost and increase the BES service life; however, the BES capacity degradation in the optimization problem to determine the optimal BES size is ignored. A summary of the literature review is presented in Table 1.

As mentioned above, the methods proposed in the literature have some shortcomings as follow: (1) The BES capacity degradation is ignored to determine the optimal BES size, which leads to unrealistic results and increase the MG total cost; (2) A non-linear model is proposed, which increases the computation time and could be stuck in a locally optimum solution; (3) A short time study is used to investigate the effect of the BES capacity degradation on BES performance and MG total cost, which decreases the accuracy of the obtained results during the planning horizon; (4) The BES service life and the relationship between the DOD and cycle life of the BES is neglected, that lead to the installed BES would not necessarily provide economic benefits; (5) The optimal replacement year of the BES is ignored, while service life and investment cost of the various BES technology is different. To overcome the mentioned shortcomings, an improved approach for optimal sizing of BES in a MG is presented in this paper.

According to the above discussions, the basic objectives and contributions of the research are as follows:

- A novel formulation for the BES sizing considering the BES service life and capacity degradation is proposed to determine the optimal BES technology and replacement year.
- A decomposition method to decompose the BES service life into two parts (cycle life and float life) is introduced to reduce the complexity of modeling and calculations.
- A MG planning method is proposed to achieve the optimal of both rated power (MW) and rated energy (MWh) of the BES considering the long-term electricity market price, generation of renewable energy resources, and demand profile of the MG to increase precision of the obtained results.
- Different BES technologies and their inherent characteristics including the cost parameters, cycle life, float life, and efficiency are considered to achieve the optimal DOD and technology of the BES.
- The modeling of the BES considering the capacity degradation for different BES technologies and DODs as a decision variable to be determined is proposed.

The remainder of the paper is formed as follows. In Section II, the formulation of the problem is presented. A test MG and main assumptions are presented in Section III to show the effectiveness and validation of the applicability of the proposed method. In Section IV, a discussion on the simulation results is presented. Finally, Section V concludes the paper.

Table 1
Summary of Literature Review.

Ref	System Considered	Time Period	Linear Model	Optimal BES DOD	BES Service Life	Replacement Year	Capacity Degradation
[16]	Connected/Islanded Microgrid	Long Time	Yes	N/A	N/A	N/A	N/A
[17]	Distribution	Short Time	Yes	N/A	N/A	N/A	N/A
[18]	Wind Farm	Short Time	No	N/A	Cycle Life	N/A	N/A
[19]	Distribution	Short Time	Yes	N/A	N/A	N/A	Considered
[20]	PV Power Plant	Short Time	Yes	N/A	Float Life	N/A	N/A
[21]	Distribution	Short Time	Yes	N/A	Cycle Life	N/A	N/A
[22]	Wind Farm	Long Time	No	N/A	Cycle Life	N/A	N/A
[23]	Distribution	Short Time	No	N/A	Cycle Life	N/A	Considered
[24]	Battery	Short Time	No	N/A	Cycle Life	N/A	Considered
[25]	Distribution	Long Time	No	N/A	Cycle Life	N/A	N/A
[26]	Islanded Microgrid	Long Time	Yes	N/A	N/A	Fixed	N/A
[27]	Hybrid Electric Vehicle	Short Time	No	Considered	Cycle Life	N/A	N/A
[28]	Shipboard	Short Time	No	N/A	Cycle Life	Fixed	N/A
[29]	Connected/Islanded Microgrid	Long Time	Yes	Considered	Cycle Life	N/A	N/A
[30]	Islanded DC Microgrid	Short Time	No	N/A	Cycle Life	N/A	Considered
Proposed Model	**Connected/Islanded Microgrid**	**Long Time**	**Yes**	**Considered**	**Both**	**Optimal**	**Considered**

2. Problem formulation

In a cost-effective MG, one of the most essential power system challenges is the optimization of the BES size, where there is a trade-off between the MG operation cost and BES investment cost [6]. A proper BES sizing can lead to a MG better performance, such as decreasing the total loss and cost, and enhancing the reliability and resilience of the MG [31]. The optimal sizing strategy depends on both rated energy (MWh) and rated power (MW), which are calculated using the BES technical characteristics and problem objectives. In this paper, the objective of the optimal BES sizing is to minimize the MG total planning cost (1), which includes the BES investment cost, the MG operation cost and the energy not supplied cost given in (2)-(4).

$$Min \quad IC + OC + C^{ENS} \tag{1}$$

$$IC = \sum_{i\in B}\left(\begin{array}{l} P_i^{BES}C_i^P + E_i^{ins}\left(C_i^E + C_i^n\right) \\ +\sum_y PW_y\left[RC_{iy} + P_i^{BES}C_i^{O\&M}\right] \end{array}\right) \tag{2}$$

$$OC = \sum_y\sum_d\sum_t PW_y\left(\begin{array}{l} \sum_{i\in G}\left[F_i\left(P_{iydt}\right)u_{iydt} + SU_i v_{iydt}\right. \\ \left. +SD_i w_{iydt}\right] + \rho_{ydt}P_{ydt}^{ex} \end{array}\right) \tag{3}$$

$$C^{ENS} = \sum_y\sum_d\sum_t PW_y P_{ydt}^{uns}\ VOLL \tag{4}$$

where P^{BES} is the BES power rating, E^{ins} is the BES installed energy rating, $F(.)$ is the cost function of dispatchable units, P is the output power of DERs, P^{ex} is the power exchanged with the utility grid, ρ is the electricity market price in the utility grid, P^{uns} is the unserved demand, $VOLL$ is the value of lost load ($/MWh), B is the set of all BES technologies, G is the set of all dispatchable units, subscript i, y, d, and t denote the DERs, year, day, and hour index, respectively. Also, u, v, and w are the binary variable that show the commitment, start-up, and shut-down state of the thermal units, respectively. The first term of the objective function, the BES investment cost IC, is comprised of the power rating cost C^P (including the balance of plant cost and power conversion system cost), energy rating cost C^E, installation cost C^n, replacement cost RC, and annual operation and maintenance cost $C^{O\&M}$ (2). The second term, the operation cost OC (3), comprises fuel cost of power generation of dispatchable units, startup cost SU, shutdown cost SD of the units inside the MG, and the cost of energy purchased from the utility grid (purchased energy times the electricity market price). By exporting the excess power of the MG to the utility grid, P^{ex} is negative, thus the operation cost is decreased. The load curtailment quantity multiplied by the value of lost load (VOLL), which called energy not supplied cost C^{ENS}, is the third term of the above objective function (4). VOLL depends on the customer type, curtailment quantities and durations, and the outage time [32]. The calculation of the investment cost is annually, whereas the calculation of the operation and energy not supplied costs are hourly and summed over the project lifetime. The present-worth cost segment $PW_y = (1+e)^{(y-1)}/(1+r)^{(y-1)}$ is used in all part of the cost function that r is the interest rate and e is the inflation rate. The objective function is subject to some MG and DERs operation constraints as follows.

2.1. Microgrid and units operation constraints

The MG operation constraints comprise power balance (5), load shedding limit (6), and power exchange limits with the utility grid (7).

$$\sum_{i\in\{G,W\}}P_{iydt} + \sum_{i\in B}\left(P_{iydt}^{ch} + P_{iydt}^{dch}\right) + P_{ydt}^{ex} + P_{ydt}^{uns} = P_{ydt}^{LD} \qquad \forall y,\ \forall d,\ \forall t \tag{5}$$

$$0 \le P_{ydt}^{uns} \le \left(P_{ydt}^{LD} - P_{ydt}^{CLD}\right) \qquad \forall y,\ \forall d,\ \forall t \tag{6}$$

$$\left|P_{ydt}^{ex}\right| \le P^{ex,max}\alpha_{ydt} \qquad \forall y,\ \forall d,\ \forall t \tag{7}$$

where $P^{ch/dch}$ is the charged/discharged power of the BES and W is the set of all nondispatchable units. The power balance equation (5) guarantees that the DERs' generated power, power exchanged with the utility grid, and power of load shedding equal MG load demand P^{LD} at all times of the planning horizon. In equation (5), the BES power is positive when discharging, negative when charging, and zero when the BES is in idle state. Moreover, when the available generated power of the local DER units in the MG and the power exchanged with the utility grid cannot supply the MG local load demand, the load shedding happens to prevent the network outages. The allowable load shedding is limited by critical load demand P^{CLD}, as in (6). Equation (7) shows the limitation of power exchange, in which $P^{ex,max}$ is the power flow limit between the MG and the utility grid and α is the binary islanding parameter. α is 1 when the MG is grid-connected and 0 when islanded. P^{ex} is negative when the excess power is exported from the MG to the utility grid, positive when the required power is imported from the utility grid to the MG, and zero otherwise.

The operation constraints of dispatchable DG units are including output power limit (8), ramping up/down (9), (10), minimum up/down time limits (11), (12), and coordination constraints (13), (14).

$$P_i^{min}u_{iydt} \le P_{iydt} \le P_i^{max}u_{iydt} \qquad \forall i\in G, \forall y, \forall d, \forall t \tag{8}$$

$$P_{iydt} - P_{iyd(t-1)} \le UR_i \qquad \forall i\in G, \forall y, \forall d, \forall t \tag{9}$$

$$P_{iyd(t-1)} - P_{iydt} \le DR_i \qquad \forall i\in G, \forall y, \forall d, \forall t \tag{10}$$

$$\sum_{h=t}^{t+UT_i-1} u_{iydh} \ge UT_i v_{iydt} \qquad \forall i\in G, \forall y, \forall d, \forall t \tag{11}$$

$$\sum_{h=t}^{t+DT_i-1}\left(1-u_{iydh}\right) \ge DT_i w_{iydt} \qquad \forall i\in G, \forall y, \forall d, \forall t \tag{12}$$

$$v_{iydt} - w_{iydt} = u_{iydt} - u_{iyd(t-1)} \qquad \forall i\in G, \forall y, \forall d, \forall t \tag{13}$$

$$v_{iydt} + w_{iydt} \le 1 \qquad \forall i\in G, \forall y, \forall d, \forall t \tag{14}$$

where $P^{min/max}$ are the minimum and maximum output power of DERs, UR/DR are the ramp up/down rate, and UT/DT are the minimum up/down time of the thermal unit i. Constraint (8) limits the thermal unit to work between the maximum and minimum output power of the unit i. The commitment state of the thermal unit is represented by a binary variable, u, which is equal to 1 when the thermal unit is in the operation state, and 0 otherwise. The increase/decrease output power of the thermal unit between two consecutive hours is limited by ramping up/down (9), (10). According to the constraints (11), (12), the thermal unit could not be shut down for at least UT hours after it was started up. Also, the thermal unit could not be started up for at least DT hours after it was shut down. In (13) and (14), the start-up and shut-down state of the thermal units are represented by binary variables v and w, respectively. v is equal to 1 when the thermal unit is started up, and 0 otherwise. Similarly, w is equal to 1 when the thermal unit is shut down, and 0 otherwise.

2.2. BES operation constraints

BES operation constraints are modeled by (15)-(21).

$$P_i^{min}z_i \le P_i^{BES} \le P_i^{max}z_i \qquad \forall i\in B \tag{15}$$

$$\gamma_i^{min} P_i^{BES} \le E_{iy}^{BES} \le \gamma_i^{max} P_i^{BES} \qquad \forall i \in B,\ \forall y \tag{16}$$

$$0 \le P_{iydt}^{dch} \le P_i^{BES} I_{iydt}^{dch} \qquad \forall i \in B,\ \forall y,\ \forall d,\ \forall t \tag{17}$$

$$-P_i^{BES}\left(1 - I_{iydt}^{dch}\right) \le P_{iydt}^{ch} \le 0 \qquad \forall i \in B,\ \forall y,\ \forall d,\ \forall t \tag{18}$$

$$SOC_{iydt} = SOC_{iyd(t-\Delta t)}(1 - \sigma_i \Delta t) - \frac{P_{iydt}^{dch}\Delta t}{\eta_i} - P_{iydt}^{ch}\Delta t \qquad \forall i \in B,\ \forall y,\ \forall d,\ \forall t \tag{19}$$

$$\left(E_{iy}^{BES} - \sum_m \frac{DOD_{im}}{100} E_{iy}^{BES} \chi_{im}\right) \le SOC_{iydt} \le E_{iy}^{BES} \qquad \forall i \in B,\ \forall y,\ \forall d,\ \forall t \tag{20}$$

$$\sum_m \chi_{im} \le z_i \qquad \forall i \in B \tag{21}$$

where E^{BES} is the BES energy rating in year y, $\gamma^{min/max}$ are the ratio of the minimum and maximum BES energy rating to the power rating, SOC is the BES state of charge, σ is the BES self-discharge rate, η is the BES round-trip efficiency, DOD is the BES DOD in percent, and subscript m denotes the DOD value index. The minimum and maximum power rating of the BES is constrained by (15). z is a binary variable that is equal to 1 when the BES of unit i is installed, and 0 otherwise. The energy rating of the BES is constrained by its limits as shown in (16). Equation (16) enables us to decouple the energy and power rating which is required in redox flow battery technology [29]. The maximum charging and discharging power of the BES in all hours is equal to the power rating of the BES (17), (18). When the BES is charging, P^{ch} is negative; also, if the BES is in the discharging state, P^{dch} is positive; Otherwise, P^{ch} and P^{dch} are equal to zero, and the BES is in idle mode. To restrict the BES operating state (charging, discharging and idle), a binary variable, I^{dch}, is employed to make sure that the BES charging/discharging state do not happen at the same time, I^{dch} is equal to 1 when the BES is in discharging state, and 0 otherwise. In (19), the BES state of charge (SOC) at time t is determined from the SOC at time $t-\Delta t$, where Δt is the charging/discharging duration, the self-discharge rate, and the charging/discharging energy at duration Δt.

In (20), the allowable SOC of the BES is limited by lower bound and upper bound. The upper bound of allowable SOC of the BES depends on the BES energy rating. The lower bound of allowable SOC of the BES is dependent on the BES energy rating and DOD. The relationship between the BES cycle life and DOD for various BES technology is given by a diagram in the BES datasheet, in which the BES cycle life is a function of the maximum DOD. In most types of batteries, when the value of DOD is low, the BES cycle life increases, but the BES usable capacity decreases, as shown in Fig. 1. Therefore, when the MG is in islanded mode, or a load shedding happens, the BES can provide less energy to the utility grid. Moreover, at high electricity market price hours, the BES can exchange less energy with the utility grid that reduces its participation in the electricity market. On the other hand, if the value of DOD is high, the cycle life of the BES decreases, except when the BES technology is vanadium redox battery (VRB) [33]. In this constraint, χ_{im} is a binary variable that is equal to 1 when the maximum DOD value of the BES is chosen and 0 otherwise. Constraint (21) guarantees that only one maximum DOD value is chosen for the BES.

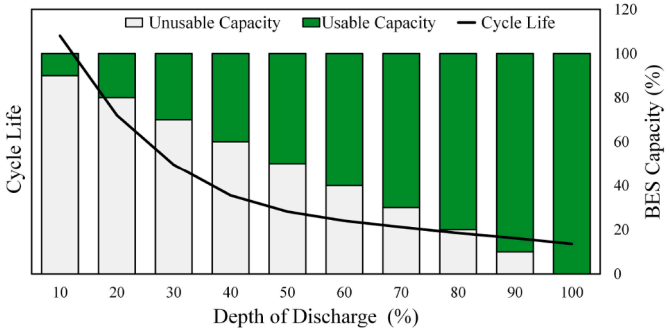

Fig. 1. The usable capacity of the BES for different DOD.

To linearize the nonlinear constraints, the big M method is employed [28], [31]. Using the big M method, the nonlinear constraint (17) is replaced with constraints (22) and (23).

$$0 \le P_{iydt}^{dch} \le P_i^{BES} \qquad \forall i \in B,\ \forall y,\ \forall d,\ \forall t \tag{22}$$

$$0 \le P_{iydt}^{dch} \le I_{iydt}^{dch} M \qquad \forall i \in B,\ \forall y,\ \forall d,\ \forall t \tag{23}$$

where M is a large positive constant. If binary variable I^{dch} is zero, P^{dch} would be zero according to (23). If I^{dch} is one, (23) is relaxed and P^{dch} is limited to the BES power rating according to (22). Here, M is set to P^{max} to ensure that the discharging power is limited to the maximum power. Similarly, the nonlinear constraint (18) is replaced by constraints (24) and (25) to linearize the constraint.

$$-P_i^{BES} \le P_{iydt}^{ch} \le 0 \qquad \forall i \in B,\ \forall y,\ \forall d,\ \forall t \tag{24}$$

$$-P_i^{max}\left(1 - I_{iydt}^{dch}\right) \le P_{iydt}^{ch} \le 0 \qquad \forall i \in B,\ \forall y,\ \forall d,\ \forall t \tag{25}$$

To linearize the nonlinear term of constraint (20), the multiplication of the continuous variable E^{BES} and binary variable χ_{im} is replaced by a new bi-linear variable LE^{BES}, i.e., $LE^{BES} = E^{BES}\chi_{im}$, and the variable LE^{BES} is described using two constraints as follows:.

$$0 \le LE_{imy}^{BES} \le M\chi_{im} \qquad \forall i \in B,\ \forall m,\ \forall y \tag{26}$$

$$E_{iy}^{BES} - M(1 - \chi_{im}) \le LE_{imy}^{BES} \le E_{iy}^{BES} + M(1 - \chi_{im}) \qquad \forall i \in B,\ \forall m,\ \forall y \tag{27}$$

where LE^{BES} is a bi-linear variable. According to (26), when χ_{im} is equal to 0, LE^{BES} would be 0. When χ_{im} is equal to 1, constraint (26) is relaxed, and according to (27), LE^{BES} would be equal to E^{BES}. Thus, the nonlinear term in (20) is linearized using (26) and (27).

2.3. BES service life constraints

The limiting factors of the BES service life are due to the corrosion processes or the maximum number of charge/discharge cycles at a specified DOD before the BES failure. Even if the BES is not used, the capacity of the BES will reduce due to the corrosion processes [34]. The corrosion processes, which is related to the cells voltage and temperature of the BES, can be estimated by float life test. Another factor that causes reduction in the capacity of the BES is cycle life, which is related to the BES DOD [35]. The calculation of the exact value of the BES service life is impossible, but two limitations are given in the datasheet of the BES: cycle life and float life. Float life is defined as the maximum life of the BES. Moreover, cycle life is defined as the maximum number of charge/discharge cycles before the BES failure which depends on the BES technology and DOD. The BES service life is determined by one of the float life or the cycle life. When one of them is reached, the BES is proposed to be replaced [15]. The BES replacement year is decomposed to two modes as follows:

1) The number of BES cycles is higher than cycle life. In this case, the optimal BES replacement year is determined by constraints (28)-(31).

$$TE_{iy}^{dch} = TE_{i(y-1)}^{dch} + \sum_d \sum_t \frac{P_{iydt}^{dch}\Delta t}{\eta_i} - TE_{i(y-1)}^{dch}\lambda_{iy} \quad \forall i \in B, \forall y \tag{28}$$

$$TE_{iy}^{dch} \le \sum_{m} N_{im}^{fail} LE_{imy}^{BES} \qquad \forall i \in B, \forall y \tag{29}$$

$$RY_{iy} = \lambda_{iy}\, y \qquad \forall i \in B, \forall y \tag{30}$$

$$RC_{iy} = C_{iy}^{r} E_{i}^{ins} \lambda_{iy} \qquad \forall i \in B, \forall y \tag{31}$$

where N^{fail} indicates the BES cycle life, RY denotes the replacement year, and C_{iy}^{r} is the BES forecasted price in year y. The discharged energy of BES in operating condition from the installation year until year y, TE^{dch}, is expressed in (28). The BES cycle life is determined based on the BES operation. In [36], a rain-flow algorithm counting, which consists of nonlinear equations, is employed to calculate the complete and incomplete cycles at each DOD. However, using non-linear equations in the BES optimal sizing model can lead to a local optimum and higher computation time [29], so this algorithm is less commonly used. Instead, the linear equations are used to determine the BES cycles [22],[28]. According to the proposed equation (29), the discharged energy should not be higher than the multiplication of the capacity of the BES and N_{im}^{fail} at all times of the planning horizon. N_{im}^{fail} is equal to the maximum number of the charge/discharge cycles of BES i with the DOD m before the BES failure. When the maximum DOD value of the BES is chosen, χ_{im} is equal to 1. As $LE_{imy}^{BES} = E_{iy}^{BES}\chi_{im}$, so LE_{imy}^{BES} equals to E_{iy}^{BES} only if the maximum DOD value m is chosen and otherwise LE_{imy}^{BES}=0. Therefore, in (29), $N_{im}^{fail} LE_{imy}^{BES}$ is non zero only if the maximum DOD value m is chosen. If the number of BES cycles are equal to the N_{im}^{fail} before the project lifetime and the BES replacement is economically advantageous, the binary variable λ will be one and the optimal replacement year is calculated by equation (30). As shown in equation (31), the BES replacement cost is calculated according to the BES forecasted price in the replacement year.

2) BES service life is higher than the float life. In this case, the replacement year is determined by constraints (32)-(34).

$$S_{iy} = S_{i(y-1)} + \beta_{iy} - S_{i(y-1)}\lambda_{iy} \qquad \forall i \in B, \forall y \tag{32}$$

$$S_{iy} \le FL_{i} \qquad \forall i \in B, \forall y \tag{33}$$

$$\beta_{iy} \le \sum_{d}\sum_{t} \frac{P_{iydt}^{dch}\Delta t}{\eta_{i}} \le M\beta_{iy} \qquad \forall i \in B, \forall y \tag{34}$$

where S is the total years of operation of the BES, β is a binary variable that shows the BES operation state of the installed BES, and FL is the float life of BES. The state-transition equation (32) shows the number of operation years of the BES from installation year until year y. The binary variable β is equal to 1 from the installation year to float life of the BES. Constraint (33) ensures that S should not exceed the float life of the BES. When the number of operation years of the BES in year y is equal to the BES float life, the BES service life is over and usage of the BES is not recommended. Therefore, according to (32), β would be 0, and the BES is removed from the planning model in year y+1, as in (34). If the BES replacement is economically advantageous in year y, the binary variable λ will be one and the BES replaces.

2.4. BES capacity degradation

The BES capacity would be reduced during the BES service life, due to the capacity degradation. The BES degradation depends on different stress factors such as temperature, current rate, and DOD. The BES degradation is mostly resulted from cycle aging and calendar aging. Cycle aging is the life reduction due to the BES charging and discharging. On the other hand, calendar aging is the BES inherent degradation over time and is mainly affected by the voltage and temperature of the cells. The effect of temperature on the calendar aging is presented in the literature. However, usually the BES employed in the MG is ventilated [37], thus the temperature is almost fixed [38]. Moreover, as the cells voltage can not be obtained easily [39] and also as the main reason of the BES capacity degradation is cycle aging, it is assumed that the BES capacity degradation is only caused by cycle aging. In addition, a linear relation between the BES degradation and cycle is considered as shown in Fig. 2 [15]. These assumptions are verified in the results presented in [40]. The BES capacity degradation is formulated by (35)-(37).

$$E_{iy}^{dch} = \frac{\sum_{d}\sum_{t} P_{iydt}^{dch}\Delta t}{\eta_{i}} \qquad \forall i \in B, \forall y \tag{35}$$

$$E_{iy}^{BES} = E_{i(y-1)}^{BES} - \sum_{m} \frac{0.2E_{i(y-1)}^{dch}\chi_{im}}{N_{im}^{fail}} + \mu_{iy} \qquad \forall i \in B, \forall y \tag{36}$$

$$\mu_{iy} = \lambda_{iy}\left(E_{i}^{ins} - E_{i(y-1)}^{BES}\right) \qquad \forall i \in B, \forall y \tag{37}$$

where E^{dch} is the discharged energy of the BES and μ is the auxiliary variable. The discharged energy in each year is determined by (35). The modeling of the BES capacity considering capacity degradation in each year for different BES technologies and N^{fail} is determined by the state-transition equation (36). This equation provides the BES energy rating in each year considering the BES capacity degradation. Also, if the rate of the BES capacity degradation due to calendar aging is available, the calendar aging would be modeled by adding to equation (36). When the BES cycle number is equal to the cycle life, the BES capacity decreases to 80% of its original amount and the BES is proposed to be replaced [15]. By replacing the BES in year y, λ is equal one, and thus the variable μ, which is equal to the BES capacity loss from the installed year to the replacement year of the BES and is calculated by equation (37), is added to equation (36) to ensure that E^{BES} in the replacement year is equal to E^{ins}. It should be noted that, the E^{BES} is equal to E^{ins} in the first year.

To linearize the multiplication of the binary variable and continuous variable in the proposed nonlinear equations (28), (31), (32), (36), (37); the big M method is employed as before.

3. Numerical simulation

3.1. Case studies and main assumptions

A MG consisting of a gas generator, a solar photovoltaic unit, and a wind turbine (WT) is used to study the proposed planning model. The characteristics of the DGs are shown in Table 2.

The hourly data of load, output power of nondispatchable units, and electricity market price are taken from the Illinois Institute of Technology MG [41]. The MG local demand details are shown in Table 3.

The capacity of the line that connects the MG to the utility grid is considered to be 10 MW. In each year, the MG is assumed to be in islanded mode for fourteen hours. The characteristics of the four considered BES technologies (including lead acid, lithium-ion (Li-ion), sodium sulfur (NaS), and nickel cadmium (NiCd)) and annual BES price reduction rate, ϑ, are presented in Table 4 [4], [25], [33], [42].

The cycle life of the different BES technologies depends on the relationship between the cycle life and DOD as represented in Table 5

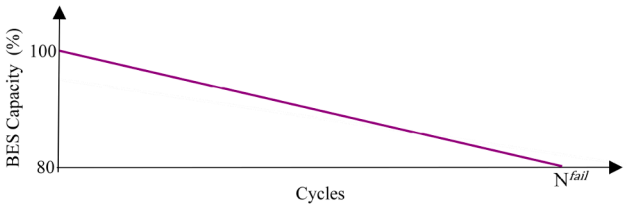

Fig. 2. BES capacity versus performed cycle numbers.

Table 2
Characteristics of Generating Units.

Unit	Type	Cost Coefficient ($/MWh)	Min-Max Capacity (MW)	Ramp Up/ Down (MW/ h)	Min Up/ Down Time (h)
1	Gas	90	1-4	3	1
2	PV	0	0-2	-	-
3	WT	0	0-5	-	-

Table 3
The MG Local Demand Details.

Load Type	Peak Load (MW)	Critical Load (%)	VOLL ($/MWh)
Commercial	8.5	30	50,000

[42], [43].

The proposed model is a mixed-integer linear programming (MILP) model that is implemented on a 2.4 GHz personal computer and solved by CPLEX 12.8. Also, to guarantee the results are globally optimal, the branch and bound method is used to solve the optimization problem [44]. The computational aspects of the method depend on the assumptions of the Cases, the optimality gap, and the planning horizon, and the highest computation time is about 27 hours for Case IV. However, in a long-time planning problem, the computation time is not as important as operation problems, and obtaining accurate results is of great importance [26].

Four different cases are defined to investigate the abilities of the proposed planning model as follows:

Case I: Optimal MG scheduling problem to minimize the total operation and energy not supplied costs without BES.

Case II: In this case, the total operation and energy not supplied costs are minimized considering the optimal BES sizing. Four scenarios introduced in Table 6 are considered to show the effectiveness of the proposed approach.

Case III: For the BESs determined in Case II, the BES capacity degradation is considered.

Case IV: The capacity degradation is taken into account and the replacement year is considered as a decision variable to be determined in the planning model.

3.2. Results and analysis

Case I: To evaluate the economic advantages of installing the BES in the MG, the BES has not been considered in this case. Therefore, the objective of the MG scheduling problem is the minimization of the total operation and energy not supplied costs. The total cost including the local dispatchable generation, energy not supplied, and energy exchanged with the utility grid costs, for project lifetime of 10 and 15 years equals $15,045,600 and $20,640,933, respectively. When the electricity market price is high, the MG's local dispatchable unit is used to supply local load demands. Most of the days, from 17:00 to 19:00, the maximum capacity of the dispatchable unit is used to supply local load demands and enhance the economic benefits due to the power exported from the MG to the utility grid; however, as the BES is not installed into the MG, the MG reliability decreases, especially during the islanded mode. Also, the operation cost of the MG increases as there is no BES to participate in the market.

Case II: In Scenario A, where the BES service life and the relationship between the BES cycle life and DOD are ignored, and for the project lifetime of 10 years, the optimal size of the BES is 5.104 MWh and 2.996 MW and the total cost is $13,396,920 that is decreased by 10.95% compared to Case I. The optimal BES technology is the cheapest one (Lead-acid), and the DOD is at its maximum (100%). When the project lifetime is increased to 15 years, the MG total cost is $17,198,060 that is decreased by 16.68% compared to Case I. However, the obtained results are not realistic because the float life and the relationship between the BES cycle life and DOD have been ignored.

In Scenario B, the BES service life modeled by constraints (28)-(34) is considered in the BES sizing, but the relationship between the BES cycle life and DOD is ignored. Also, it is assumed that the BES could not be replaced, and the value of DOD is at its maximum. In 10-Year planning horizon, the optimal BES sizing is 2.602 MWh and 1.978 MW. The total cost is $14,230,110, the optimal BES technology is Li-ion, and the maximum DOD is 80%. The MG total cost is decreased by 5.42% compared to Case I. For 15-Year planning horizon, the optimal BES technology is NaS and the MG total cost is decreased by 3.54% compared to the Case I. By increasing the planning horizon, the investment on the more expensive BES technology with higher service life could provide an economic benefit to the MG via participation in the electricity market by storing energy at off-peak hours and discharging the stored energy at peak hours and thus reducing the energy not supplied due to the load shedding in the MG.

In Scenario C, the relationship between the BES cycle life and DOD for optimal selection of DOD is considered. Also, it is assumed that the BES could not be replaced. In this scenario, the optimal BES DOD for 10-

Table 5
BES Cycle Life Versus DOD (Temperature 20°C).

DOD (%)	Lead-acid	Li-ion	NaS	NiCd
10	-	170000	120000	-
20	3000	48000	39000	7650
30	2075	21050	20000	4900
40	1500	11400	12800	3300
50	1175	6400	9000	2300
60	1000	4150	6650	1600
65	940	3500	5800	1350
70	900	3000	5200	1150
75	825	2700	4650	975
80	775	2500	4200	875
85	700	-	3800	780
90	675	-	3550	700
95	600	-	3250	-
100	550	-	3100	-

Table 6
Various Scenarios Pertaining to Case II.

Scenario	Service life	Optimal DOD	Replacement
A	N/A	N/A	N/A
B	Considered	N/A	N/A
C	Considered	Considered	N/A
D	Considered	Considered	Considered

Table 4
BES Technologies Characteristics.

Technology	Round-trip Efficiency (%)	Float Life (year)	Daily Self-discharge (%)	Power Rating Cost ($/kW)	Energy Rating Cost ($/kWh)	Installation Cost ($/kWh)	Operation and Maintenance Cost ($/kW-year)	β (%)
NaS	75	15	0	360	520	40	10	4.6
Li-ion	95	10	0.2	320	360	15	5	5.5
Lead-acid	72	5	0.2	300	170	30	10	2.2
NiCd	80	20	0.3	500	350	50	20	3

Table 7
Numerical Simulation Results for Case II Scenario C.

Maximum DOD (%)	65	70	75	80	85	90	95	100
IC($)	3,212,847	3,050,583	2,909,954	2,787,135	2,678,531	2,581,825	2,512,716	2,471,266
C^{ENS}($)	590,451	590,451	590,451	590,451	590,451	590,451	590,451	590,451
OC($)	16,391,440	16,396,659	16,411,323	16,468,207	16,602,446	16,709,817	16,798,031	16,848,834
Total Cost($)	20,194,738	20,037,693	19,911,728	19,845,793	19,871,428	19,882,093	19,901,198	19,910,551
Power Rating (MW)	1.978	1.978	1.978	1.978	1.978	1.978	1.978	1.978
Energy Rating (MWh)	4.057	3.767	3.516	3.296	3.102	2.930	2.806	2.732

Year and 15-Year project lifetime are 75% and 80%, respectively; compared to Scenario B, which the amount of DOD is assumed to be fixed at its maximum. The MG total cost reduction for 10-Year and 15-Year project lifetime are 0.22% and 0.33%, respectively. The NaS BES cycle life equals 4200 at 80% DOD. Thus, the economic benefit of MG due to the BES participation in the electricity market increases. To evaluate the effect of DOD on the MG total cost and confirm the ability of the BES planning model in determining the optimal amount of DOD, the numerical simulation is carried out for different DOD amount of NaS BES for 15-Year planning horizon. As shown in Table 7, the MG total cost reduces as the DOD increases until the optimal maximum DOD, i.e., 80%, is reached by the proposed planning model.

As shown in Fig. 1, by increasing the maximum DOD values of the BES, the BES useable capacity increases and the BES cycle life decreases and thus the optimal BES size and its investment cost decreases. However, due to reduction in the BES cycle life, the MG operation cost increases. On the other hand, by reducing the maximum DOD values of the BES, the BES useable capacity reduces and so the optimal BES size and its investment cost increases. Therefore, high or low values of DOD do not necessarily provide economic benefit and its optimal value should be determined by the optimal planning model.

In Scenario D, the BES service life, optimal DOD, and optimal replacement year are considered. When the project lifetime is 10 years, the optimal BES technology is Li-ion, and the optimal DOD is 75%. The installed BES do not need to be replaced during the planning horizon. Since the considered Li-ion float life is 10 years and the number of BES cycles during the planning horizon is less than N^{fail} at DOD of 75%. For project lifetime of 15 years, the optimal BES technology is Li-ion and the optimal replacement year is 9. It is worth noting that in spite of the higher service life of the NaS technology with respect to the Li-ion technology, using the Li-ion technology and replacing it in year 9 is more economical than using the NaS technology without any replacement mostly due to its higher power and energy rating cost. The MG total cost compared to Scenario C, in which the BES replacement has not been considered, is decreased by 4.1%. Moreover, the energy not supplied during the planning horizon is decreased from 14.6 MWh to 0 MWh. To evaluate the effect of replacement year on the MG total cost and to confirm the ability of the BES planning model in determining the optimal BES replacement year, the numerical simulation is carried out for different replacement years of Li-ion battery for 15-Year planning horizon. As shown in Fig. 3, the total cost is minimum in year 9 which validates the results obtained by the proposed model.

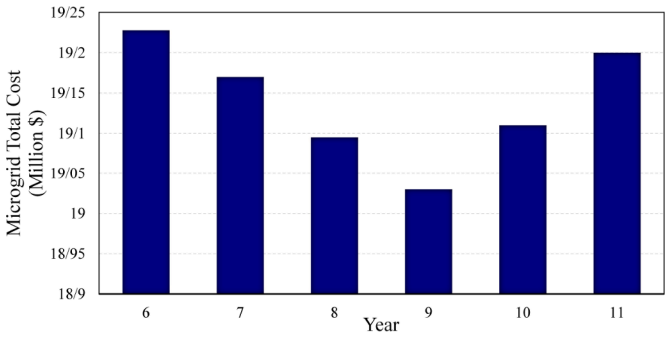

Fig. 3. MG total cost for different replacement years for Scenario D of Case II and 15-Year planning horizon.

Table 8 summarizes the costs and optimal BES technology, power and energy rating, DOD, and replacement year in the scenarios of Case II.

As shown in Table 8, Scenario A has the lowest total cost. But, it should be noted that the result of Scenario A is not realistic as the service life of the battery is assumed to be lifetime. Among the scenarios in which the service life is also considered, Scenario D has the lowest total cost which validates the ability of the proposed model to optimally determine the BES size, technology, DOD, and replacement year in a such way that the total cost is minimized. The effect of the BES capacity degradation has not yet been considered.

Fig. 4 shows the profiles of DERs output power and power exchanged with the utility grid. As shown, the BES is charged at off-peak hours to be used at peak hours for satisfying the load or sell power to the utility grid. Also, the gas generator is used to supply the load and sell the surplus power to the utility grid at peak hours to gain the economic benefits.

Case III: In this case, the effect of ignoring the BES capacity degradation on the accuracy of the obtained results of Case II is investigated. Also, it is assumed that the planning horizon is 15 years. As shown in Table 9, if the same batteries determined in four scenarios of Case II are employed, the BES provides less energy due to the BES capacity degradation and thus the energy not supplied cost and operation cost of the MG increase. Due to ignoring the BES service life and capacity

Table 8
Numerical Simulation Results for Case II.

Scenario	A		B		C		D	
Project lifetime (year)	10	15	10	15	10	15	10	15
IC($)	2,172,725	2,802,060	1,736,769	2,471,266	1,799,443	2,787,135	1,799,443	3,339,297
C^{ENS}($)	0	0	430,392	590,451	430,392	590,451	430,392	0
OC($)	11,224,195	14,396,000	12,062,949	16,848,834	11,969,560	16,468,207	11,969,560	15,694,887
Total Cost($)	13,396,920	17,198,060	14,230,110	19,910,551	14,199,395	19,845,793	14,199,395	19,034,184
BES Technology	Lead-acid	Lead-acid	Li-ion	NaS	Li-ion	NaS	Li-ion	Li-ion
Power Rating (MW)	2.996	2.996	1.978	1.978	1.978	1.978	1.978	2.996
Energy Rating (MWh)	5.104	7.780	2.602	2.732	2.776	3.296	2.776	3.943
Maximum DOD (%)	100	100	80	100	75	80	75	80
Replacement Year	-	-	-	-	-	-	-	9

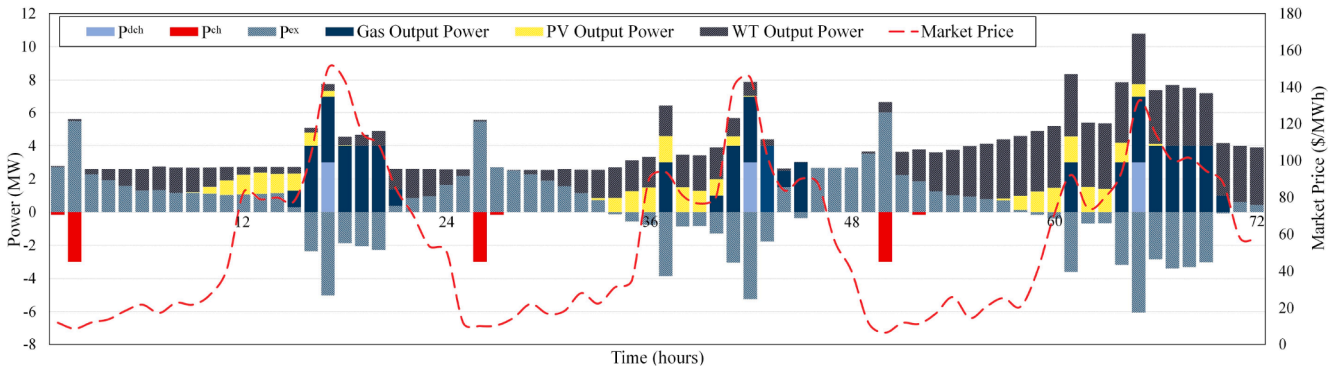

Fig. 4. The profiles of DERs output power and power exchanged with utility grid for Scenario D of Case II and 15-Year.

Table 9
Numerical Simulation Results for Case III.

Scenario	A	B	C	D
IC($)	2,802,060	2,471,266	2,787,135	3,339,297
C^{ENS}($)	1,779,965	685,609	761,001	136,422
OC($)	17,271,252	17,007,926	16,632,260	15,911,693
Total Cost($)	21,853,277	20,164,801	20,180,396	19,387,412

Table 10
Numerical Simulation Results for Case IV.

Project lifetime (year)	10	15
IC($)	2,011,117	3,608,976
C^{ENS}($)	438,004	12,107
OC($)	11,902,630	15,677,660
Total Cost($)	14,351,751	19,298,743
BES Technology	Li-ion	Li-ion
Power Rating (MW)	1.978	2.996
Energy Rating (MWh)	3.364	4.466
DOD (%)	70	80
Replacement Year	-	9

degradation in Scenario A, the MG total cost is increased by 5.87% compared to Case I thus the chosen BES of Scenario A would not provide economic benefit. For other the scenarios, ignoring the effect of the BES capacity degradation leads to unrealistic results and the MG total cost would be much higher in reality than the total cost obtained by the optimization problem. Therefore, in order to increase the accuracy of the obtained results, the effect of the BES capacity degradation on the BES operation and the total cost should be considered.

Case IV: In this case, in addition to the assumptions made in Scenario D of Case II, the BES capacity degradation is also considered to improve the accuracy of the modeling and optimal selection of the BES. As shown in Table 10, the MG total cost reduction compared to Case I for 10-Year and 15-Year project lifetimes are 4.62% and 6.5%, respectively. For 15-Year project lifetime, the optimal technology is Li-ion and the replacement year is 9. Although the NaS technology has more service life, it has more energy rating cost, power rating cost, and investment cost.

As shown in Fig. 5, the BES capacity due to the cycle aging reduces during the BES lifetime and the BES could store less energy at off-peak hours to be used at peak hours, which increases the MG operation cost during the planning horizon. Moreover, the BES provides less energy to the loads in the islanded mode. Therefore, the energy not supplied cost would be increased. The Li-ion battery state of health (SOH) decreases below 80% in year 9, thus the BES is replaced in year 9, the BES replacement cost is $1,027,183. Because of considering the BES capacity degradation in the proposed planning model, the MG total cost is higher than Scenario D of Case II. However, comparing the results of Cases III with Case IV shows the ability of the proposed model to determine the optimal BES and reduce the MG total cost.

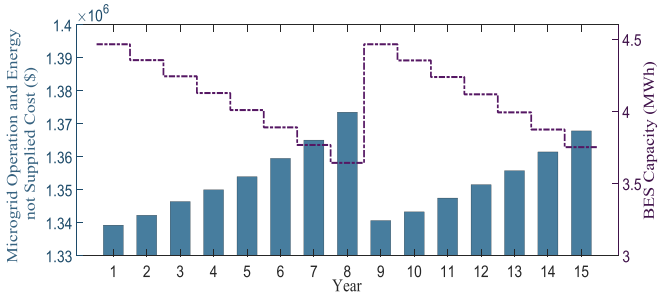

Fig. 5. MG operation cost and the BES capacity during the planning horizon.

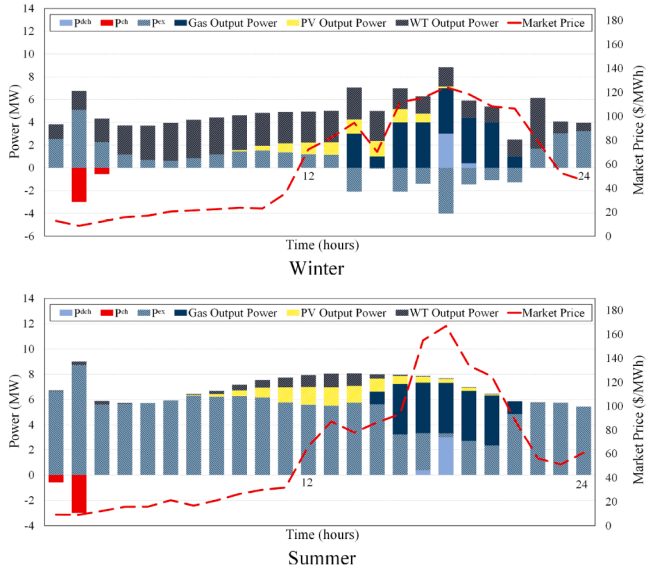

Fig. 6. The profiles of DERs output power and power exchanged with the utility grid for Case IV for a typical summer and winter day.

The profiles of DERs output power and power exchanged with the utility grid for a typical summer and winter day of the first year, are shown in Fig. 6. In winter, due to the increase in wind speed, the WT has a better performance and thus less power is imported from the utility grid. As the wind speed decreases in summer, the WT output power also decreases, thus the MG buy more power from the utility grid, which increases the MG operation cost. Developing the PV units in the MG understudy could decrease the MG operation cost because the PV output power pattern is similar to the MG load demand and electricity market price.

4. Discussion

According to the obtained results from the numerical simulations, the following could be concluded:

- Ignoring the effect of the BES capacity degradation and the BES service life in the planning framework leads to unrealistic results in which the installed BES does not necessarily provide economic benefits to the MG.
- In the optimal BES sizing problem for the MG, considering the optimal BES technology and DOD can significantly reduce the MG total cost.
- Installing the BES into the MG could decrease the operation cost and increase the MG reliability by reducing the load shedding in the islanded mode.
- Considering the possibility of replacing the BES during the planning horizon, the installation of an inexpensive BES that has low service life could be more economical than the one with high service life.
- Due to the BES capacity degradation during the planning horizon, a short time study (e.g., one-day or one-year) to determine the optimal BES reduces the accuracy and the practicality of the obtained results.

5. Conclusion

In this paper, by considering the BES service life and capacity degradation for the MG planning problem, an improved approach was proposed to calculate the optimal BES size, technology, DOD, and replacement year. With the aim of MGs total cost reduction, the problem has been formulated using the MILP method. To evaluate the effectiveness and the practicality of the proposed method, various scenarios and case studies were investigated. Numerical simulations showed that the results of the planning model would not be economical if the BES service life is ignored during the planning horizon. Also, it was found that the longer service life of the BES does not necessarily provide more economic benefits to the MG. Moreover, the impact of the BES capacity degradation on the BES operation and the MG total cost was investigated. Due to the BES capacity degradation, the BES capacity decreases during the planning horizon and provides less energy in islanded mode and thus the benefits of BES participation in the electricity market price reduces. Therefore, by considering the capacity degradation in the BES sizing, more economic benefits can be achieved. Using the proposed planning model, the total cost of the MG under study for the 10-Year and 15-Year planning horizon can be reduced by 4.62% and 6.5%, respectively. Therefore, the proposed model is a viable solution to BES size problem in a MG.

CRediT authorship contribution statement

Mohammad Amini: Conceptualization, Methodology, Validation, Formal analysis, Investigation, Resources, Data curation, Writing - original draft, Writing - review & editing, Visualization. **Amir Khorsandi:** Conceptualization, Supervision, Investigation, Writing - original draft, Writing - review & editing, Project administration. **Behrooz Vahidi:** Supervision, Writing - original draft. **Seyed Hossein Hosseinian:** Supervision, Writing - original draft. **Ali Malakmahmoudi:** Writing - original draft.

Declaration of competing interest

The authors declare that they have no known competing financial interests or personal relationships that could have appeared to influence the work reported in this paper.

References

[1] V.C. Gungor, D. Sahin, T. Kocak, S. Ergut, C. Buccella, C. Cecati, G.P. Hancke, Smart grid technologies: Communication technologies and standards, IEEE Trans. Ind. Inf. 7 (4) (2011) 529–539.
[2] D.T. Ton, M.A. Smith, The us department of energy's microgrid initiative, The Electric. J. 25 (8) (2012) 84–94.
[3] H. Chen, T.N. Cong, W. Yang, C. Tan, Y. Li, Y. Ding, Progress in electrical energy storage system: a critical review, Progr. Natur. Sci. 19 (3) (2009) 291–312.
[4] X. Luo, J. Wang, M. Dooner, J. Clarke, Overview of current development in electrical energy storage technologies and the application potential in power system operation, Appl. Energy 137 (2015) 511–536.
[5] H. Beltran, E. Bilbao, E. Belenguer, I. Etxeberria-Otadui, P. Rodriguez, Evaluation of storage energy requirements for constant production in pv power plants, IEEE Trans. Ind. Electron. 60 (3) (2012) 1225–1234.
[6] S. Chen, H.B. Gooi, M. Wang, Sizing of energy storage for microgrids, IEEE Trans. Smart Grid 3 (1) (2011) 142–151.
[7] T. Kerdphol, Y. Qudaih, Y. Mitani, Optimum battery energy storage system using pso considering dynamic demand response for microgrids, Int. J. Electric. Power Energy Syst. 83 (2016) 58–66.
[8] M.A. Abdulgalil, M. Khalid, Enhancing the reliability of a microgrid through optimal size of battery ess, IET Generat. Transm. Distribut. 13 (9) (2019) 1499–1508.
[9] Q. Fu, L.F. Montoya, A. Solanki, A. Nasiri, V. Bhavaraju, T. Abdallah, C.Y. David, Microgrid generation capacity design with renewables and energy storage addressing power quality and surety, IEEE Trans. Smart Grid 3 (4) (2012) 2019–2027.
[10] B. Zhang, P. Dehghanian, M. Kezunovic, Optimal allocation of pv generation and battery storage for enhanced resilience, IEEE Trans. Smart Grid 10 (1) (2017) 535–545.
[11] F. Mohammadi, H. Gholami, G.B. Gharehpetian, S.H. Hosseinian, Allocation of centralized energy storage system and its effect on daily grid energy generation cost, IEEE Trans. Power Syst. 32 (3) (2016) 2406–2416.
[12] U.T. Salman, F.S. Al-Ismail, M. Khalid, Optimal sizing of battery energy storage for grid-connected and isolated wind-penetrated microgrid, IEEE Access 8 (2020) 91129–91138.
[13] S. Wogrin, D.F. Gayme, Optimizing storage siting, sizing, and technology portfolios in transmission-constrained networks, IEEE Trans. Power Syst. 30 (6) (2014) 3304–3313.
[14] M. Sanjareh, M. Nazari, Coordination of energy storage system, pvs and smart lighting loads to reduce required battery size for improving frequency response of islanded microgrid, Sustain. Energy Grid. Netw. (2020) 100357.
[15] Y. Yang, H. Li, A. Aichhorn, J. Zheng, M. Greenleaf, Sizing strategy of distributed battery storage system with high penetration of photovoltaic for voltage regulation and peak load shaving, IEEE Trans. Smart Grid 5 (2) (2013) 982–991.
[16] H. Lotfi, A. Khodaei, Ac versus dc microgrid planning, IEEE Trans. Smart Grid 8 (1) (2015) 296–304.
[17] S. Massucco, P. Pongiglione, F. Silvestro, M. Paolone, F. Sossan, Siting and sizing of energy storage systems: Towards a unified approach for transmission and distribution system operators for reserve provision and grid support, arXiv preprint arXiv:2004.09146 (2020).
[18] I.N. Moghaddam, B.H. Chowdhury, S. Mohajeryami, Predictive operation and optimal sizing of battery energy storage with high wind energy penetration, IEEE Trans. Ind. Electron. 65 (8) (2017) 6686–6695.
[19] J. Mao, M. Jafari, A. Botterud, Pleanning low-carbon distributed power systems: Evaluating the role of energy storage, arXiv preprint arXiv:2009.09325 (2020).
[20] A. Saez-de Ibarra, A. Milo, H. Gaztanaga, V. Debusschere, S. Bacha, Co-optimization of storage system sizing and control strategy for intelligent photovoltaic power plants market integration, IEEE Trans. Sustain. Energy 7 (4) (2016) 1749–1761.
[21] X. Ke, N. Lu, C. Jin, Control and size energy storage systems for managing energy imbalance of variable generation resources, IEEE Trans. Sustain. Energy 6 (1) (2014) 70–78.
[22] I.N. Moghaddam, B.H. Chowdhury, M. Doostan, Optimal sizing and operation of battery energy storage systems connected to wind farms participating in electricity markets, IEEE Trans. Sustain. Energy (2018).
[23] Y. Zhang, Y. Xu, H. Yang, Z.Y. Dong, R. Zhang, Optimal whole-life-cycle planning of battery energy storage for multi-functional services in power systems, IEEE Trans. Sustain. Energy (2019).
[24] W. Diao, S. Saxena, M. Pecht, Accelerated cycle life testing and capacity degradation modeling of licoo2-graphite cells, J. Power Sour. 435 (2019) 226830.
[25] T. Sayfutdinov, C. Patsios, J.W. Bialek, D.M. Greenwood, P.C. Taylor, Incorporating variable lifetime and self-discharge into optimal sizing and technology selection of energy storage systems, IET smart grid 1 (1) (2018) 11–18.
[26] H. Alharbi, K. Bhattacharya, Stochastic optimal planning of battery energy storage systems for isolated microgrids, IEEE Trans. Sustain. Energy 9 (1) (2017) 211–227.
[27] S. Xie, X. Hu, Q. Zhang, X. Lin, B. Mu, H. Ji, Aging-aware co-optimization of battery size, depth of discharge, and energy management for plug-in hybrid electric vehicles, J. Power Sour. 450 (2020) 227638.
[28] A. Boveri, F. Silvestro, M. Molinas, E. Skjong, Optimal sizing of energy storage systems for shipboard applications, IEEE Trans. Energy Conver. 34 (2) (2018) 801–811.
[29] I. Alsaidan, A. Khodaei, W. Gao, A comprehensive battery energy storage optimal sizing model for microgrid applications, IEEE Trans. Power Syst. 33 (4) (2017) 3968–3980.

[30] J.-O. Lee, Y.-S. Kim, T.-H. Kim, S.-I. Moon, Novel droop control of battery energy storage systems based on battery degradation cost in islanded dc microgrids, IEEE Access 8 (2020) 119337–119345.
[31] H. Xie, X. Teng, Y. Xu, Y. Wang, Optimal energy storage sizing for networked microgrids considering reliability and resilience, IEEE Access 7 (2019) 86336–86348.
[32] A. Khodaei, S. Bahramirad, M. Shahidehpour, Microgrid planning under uncertainty, IEEE Trans. Power Syst. 30 (5) (2014) 2417–2425.
[33] K. Mongird, V.V. Viswanathan, P.J. Balducci, M.J.E. Alam, V. Fotedar, V. S. Koritarov, B. Hadjerioua, Energy storage technology and cost characterization report. Technical Report, Pacific Northwest National Lab.(PNNL), Richland, WA (United States), 2019.
[34] G. He, Q. Chen, C. Kang, P. Pinson, Q. Xia, Optimal bidding strategy of battery storage in power markets considering performance-based regulation and battery cycle life, IEEE Trans. Smart Grid 7 (5) (2015) 2359–2367.
[35] Y. Yang, Q. Ye, L.J. Tung, M. Greenleaf, H. Li, Integrated size and energy management design of battery storage to enhance grid integration of large-scale pv power plants, IEEE Trans. Ind. Electron. 65 (1) (2017) 394–402.
[36] X. Ke, N. Lu, C. Jin, Control and size energy storage systems for managing energy imbalance of variable generation resources, IEEE Trans. Sustain. Energy 6 (1) (2014) 70–78.
[37] D.-I. Stroe, M. Swierczynski, A.-I. Stroe, R. Laerke, P.C. Kjaer, R. Teodorescu, Degradation behavior of lithium-ion batteries based on lifetime models and field measured frequency regulation mission profile, IEEE Trans. Ind. Appl. 52 (6) (2016) 5009–5018.
[38] B. Xu, A. Oudalov, A. Ulbig, G. Andersson, D.S. Kirschen, Modeling of lithium-ion battery degradation for cell life assessment, IEEE Trans. Smart Grid 9 (2) (2016) 1131–1140.
[39] L. De Sutter, G. Berckmans, M. Marinaro, J. Smekens, Y. Firouz, M. Wohlfahrt-Mehrens, J. Van Mierlo, N. Omar, Comprehensive aging analysis of volumetric constrained lithium-ion pouch cells with high concentration silicon-alloy anodes, Energies 11 (11) (2018) 2948.
[40] K. Thirugnanam, E.R.J. TP, M. Singh, P. Kumar, Mathematical modeling of li-ion battery using genetic algorithm approach for v2g applications, IEEE Trans. Energy Conver. 29 (2) (2014) 332–343.
[41] [online].available: http://iitmicrogrid.net/microgrid.aspx. [accessed: 21-mar-2015].
[42] [online].available: https://www.saftbatteries.com/.
[43] [online].available: https://www.crownbattery.com/.
[44] T. Ding, R. Bo, F. Li, H. Sun, A bi-level branch and bound method for economic dispatch with disjoint prohibited zones considering network losses, IEEE Trans. Power Syst. 30 (6) (2014) 2841–2855.